

Supporting Information

Manipulating the surface states of BiVO₄ through electrochemical reduction for enhanced PEC water oxidation

Peixin Yang¹, Huihui Shi², Hangfei Wu¹, Duohuan Yu¹, Lu Huang², Yali Wu², Xiangnan Gong³, Peng Xiao^{1}, Yunhuai Zhang^{2*}*

1. Chongqing Key Laboratory of Soft Condensed Matter Physics and Smart Materials, College of Physics, Chongqing University, Chongqing 401331, China

2. College of Chemistry and Chemical Engineering, Chongqing University, Chongqing 401331, China

3. Analytical and Testing Center, Chongqing University, Chongqing, 401331, China.

** Corresponding Authors: xiaopeng@cqu.edu.cn; zyh2031@cqu.edu.cn*

Methods:

Mott-Schottky measurements: The donor density (N_D) associated with BiVO₄ photoanodes was estimated using the Mott-Schottky equation shown below:

$$\frac{A^2}{C_{SC}^2} = \frac{2}{qN_D\epsilon_r\epsilon_0} \left(E - E_{FB} - \frac{k_B T}{e} \right)$$

where A is semiconductor/electrolyte interface contact area, C_{SC} is the capacitance of space charge layer measured under dark, E is applied potential vs. Ag/AgCl, E_{FB} is the flat band potential, k_B is Boltzmann constant, T is absolute temperature, e is an elementary charge, ϵ_r is the relative permittivity of the BiVO₄ (~ 68), ϵ_0 is the permittivity of the vacuum, q is the electronic charge (1.602×10^{-19} C).

IPCE: incident photon-to-current conversion efficiency (IPCE) was calculated from following Equation:

$$IPCE = \frac{1024 \times j_{ph}}{\lambda \times P_{light}} \times 100\%$$

where I is the photocurrent density; λ is the wavelength of incident light.

ABPE: The applied bias photocurrent conversion efficiency (ABPE) of photoanodes computed using the following equation;

$$ABPE = \frac{J_{ph} \times (1.23 - |V_{bias}|)}{P_{total}} \times 100\%$$

where J_{ph} is the photocurrent density obtained under an applied bias (V_{bias}), and P_{total} is the incident illumination power density.

Calculation of maximum photocurrent (J_{abs})

The energy of a single photon can be expressed as

$$E = \frac{h \times c}{\lambda}$$

where $E(\lambda)$ is the photon energy, h is Planck's constant (6.626×10^{-34} J s), c is the speed of light (3×10^8 m s⁻¹) and λ is the photon wavelength (m).

The solar photon flux reads as

$$Flux(\lambda) = P(\lambda)/E(\lambda)$$

where Flux (λ) is the solar photon flux (m⁻²s⁻¹nm⁻¹), $P(\lambda)$ is the solar power flux (Wm⁻²nm⁻¹)¹

The maximum photocurrent density under A.M 1.5G solar illumination, J_{abs} (mA cm⁻²) is then expressed as

$$J_{abs} = e \times \left(\int_{\lambda_1}^{\lambda_2} (A \times Flux(\lambda) d\lambda) \right)$$

where A is optical absorbance, λ_1 is the absorption edge (~520 nm), λ_2 is the lower limit of the measured solar spectrum (290 nm), and e is the elementary charge (1.602×10^{-19} C). Therefore, the calculated J_{abs} for all the BiVO₄ photoanodes is found to be 5.2 mA cm².

η_{sep} and η_{inj} calculation :

$$\eta_{sep} = \frac{J_{hole}}{J_{abs}}$$

$$\eta_{inj} = \frac{J_{ph}}{J_{hole}}$$

Herein, J_{ph} is the photocurrent measured in 0.2 M Na₂SO₄. J_{hole} is the photocurrent measured in 0.2 M Na₂SO₄ and 0.2 M Na₂SO₃ mixed solution.

Characterization Details:

Structural and phase analyses with X-ray diffraction (XRD) were achieved with a

Shimadzu ZD-3AX using Cu K α ($\lambda = 1.5418 \text{ \AA}$) radiation. Light absorption properties of semiconductor materials were acquired with a UV-vis spectrometer (UV-3600, Shimadzu). X-ray photoelectron spectroscopy (XPS, Thermo Scientific, ESCALAB 250Xi) was employed to characterize the surface chemical states, and the quantitative chemical component analyses of the samples were performed using Thermo Scientific Avantage Software. Field-emission scanning electron microscopy (FE-SEM, Nova 400 Nano-SEM) and transmission electron microscopy (TEM, Talos F200S) are used to characterize the morphology and microstructure of samples. Photoluminescence spectra under 375 nm excitation were carried out using the spectrofluorometer FLS 920 (Edinburgh Instruments) equipped with xenon lamps. Raman spectra were measured on Raman Spectrometer (LabRAM HR Evolution) with 532 nm laser.

Photoelectrochemical Details:

All the photoelectrochemical measurements were carried out through an electrochemical workstation (Zahner Zennium and PP211, Germany). All the PEC performances were performed in a three-electrode system. A Ag/AgCl (saturated KCl solution) electrode, Pt electrode and the prepared photoanodes were used as the reference, counter and working electrodes respectively, the 0.2 M Na₂SO₄ solution (pH=7) was used as the electrolyte. Solar light irradiation was simulated by xenon lamp (HSX-F300, China) equipped with AM 1.5G filter. Its intensity was set at 1 Sun (100 mW cm⁻²) by a light power meter (CEL-FZ-A, China). The front-side illumination (sample side) were adopted in all the photoelectrochemical measurements. A mixed solution of 0.2 M Na₂SO₃ and 0.2 M Na₂SO₄ was used as a hole scavenger for the

measurements of separation efficiency (η_{sep}) and charge transfer efficiency (η_{ct}). According to the Nernst equation (25 °C): $E_{\text{RHE}} = E_{\text{Ag/AgCl}} + 0.059 \text{ pH} + 0.197$, the potentials vs Ag/AgCl were transformed to the potentials vs reversible hydrogen electrode (RHE). Photocurrent vs. voltage (J-V) characteristics were recorded by scanning potential from 0.2-1.4 V_{RHE} with scan rate of 10 mV s^{-1} . Photoelectrochemical impedance spectroscopy (PEIS) measurements were carried out in the frequency range from 0.1 Hz to 10 kHz with an AC voltage amplitude of 15 mV. Mott-Schottky (M-S) spectra were carried out in the voltage window of 0.7-1.3 V_{RHE} in the dark at the frequency of 1 kHz. IMPS measurements were conducted using a white light-emitting diode (LED: LSW-2) with a light intensity of 100 mW cm^{-2} controlled by a light source driver (pp211). The frequency range of 0.1 Hz to 10 kHz was determined to acquire the measured result.

Computational method:

The first principle calculations were performed by Vienna Ab initio Simulation Package (VASP)^[1] with the projector augmented wave (PAW) method^[2]. The exchange-functional was treated using the Perdew-Burke-Ernzerhof (PBE) functional^[1]. The calculations were performed in a spin-polarized manner. The cut-off energy of the plane-wave basis was set at 500 eV. For the optimization of both geometry and lattice size, the Brillouin zone integration was performed with $3 \times 3 \times 2$ Monkhorst-Pack k-point sampling. The self-consistent calculations apply a convergence energy threshold of 10^{-5} eV. The equilibrium geometries and lattice constants were optimized with maximum stress on each atom within 0.02 eV/\AA . The surface energy (E_s) was

calculated by the following equation,

$$E_s = \frac{1}{2A}(E_{slab} - E_{bulk})$$

where E_{slab} denotes the total energy of the surface slab, E_{bulk} is the total energy of a space filling bulk slab^[3]. Where A is the surface unit cell area, E_{slab} is the energy of cleaved surface.

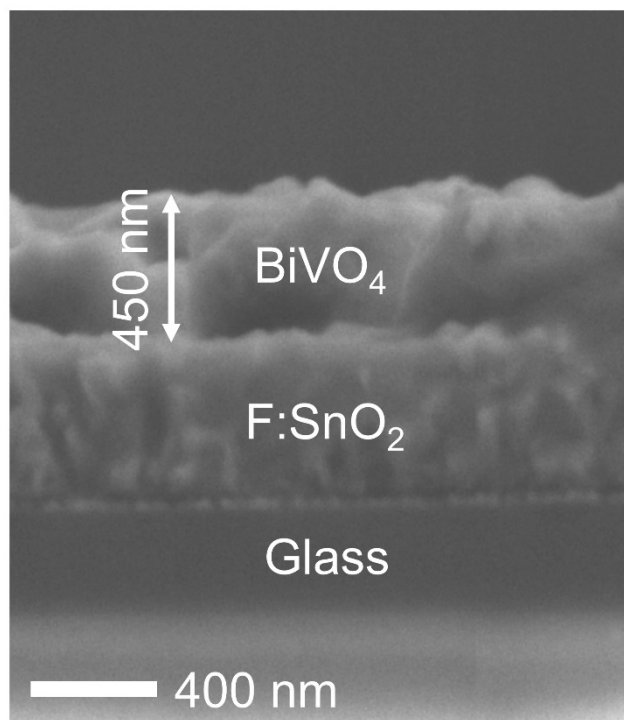


Figure S1 The cross-sectional part of the BiVO₄ photoanode.

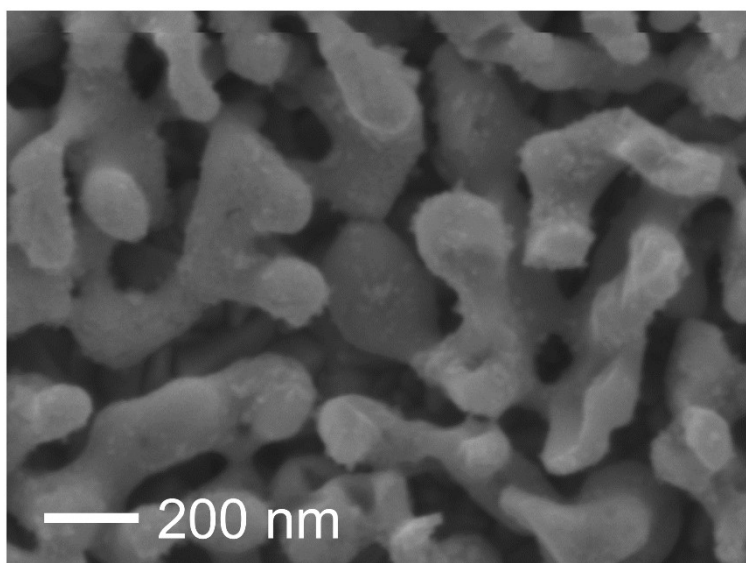


Figure S2 SEM image of -0.6/BVO photoanode.

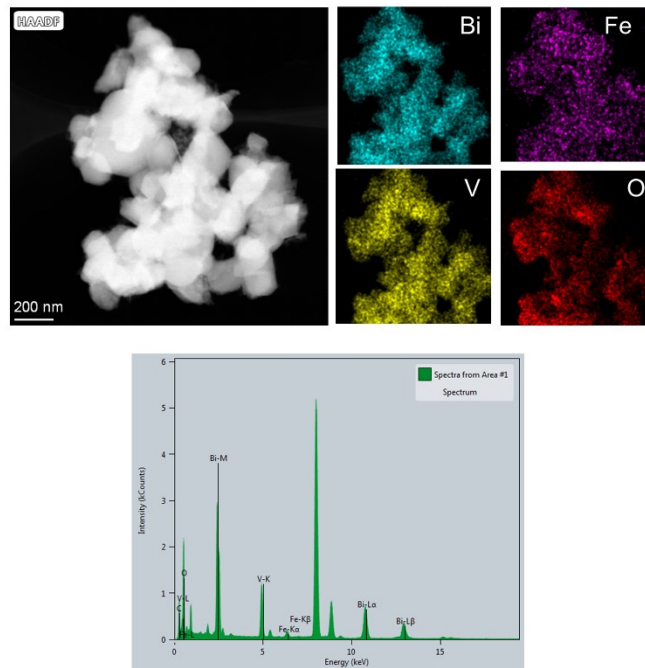


Figure S3 TEM mapping and EDX spectrum of -0.8/BVO/Fe

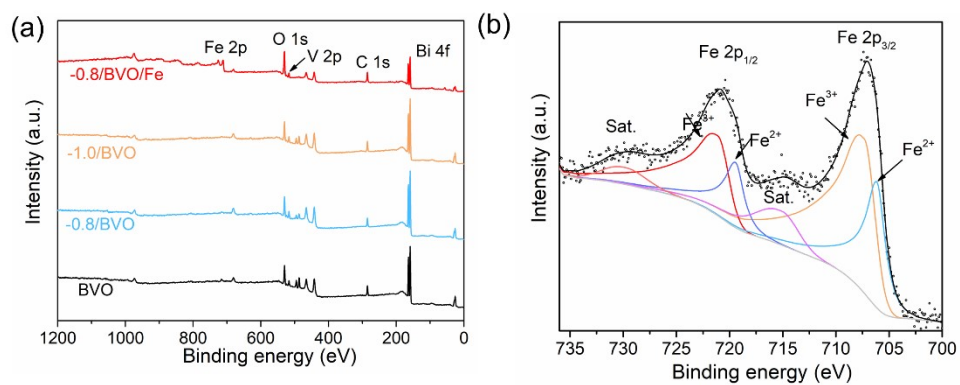


Figure S4. XPS spectra of (a) full spectrum survey of different samples and (b) Fe 2p for -0.8/BVO/Fe

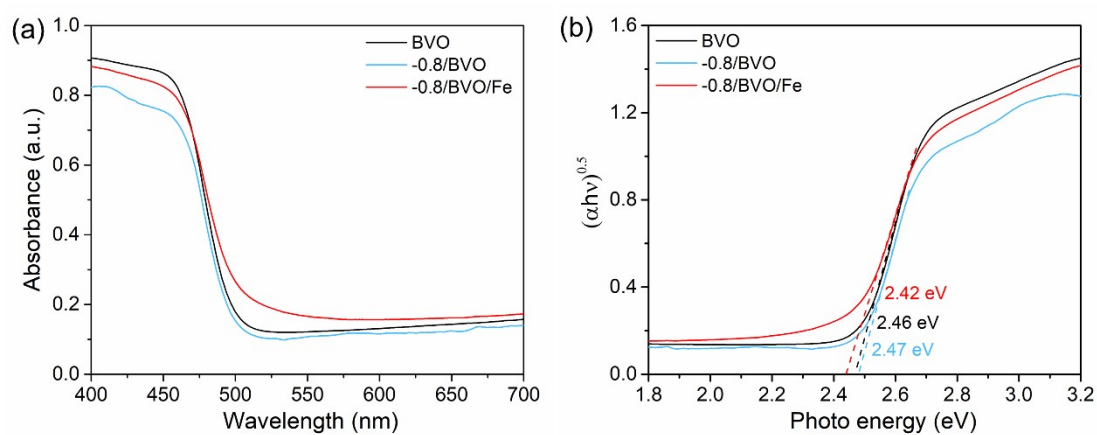


Figure S5. (a) UV-vis absorption spectra and (b) Tauc plots of samples.

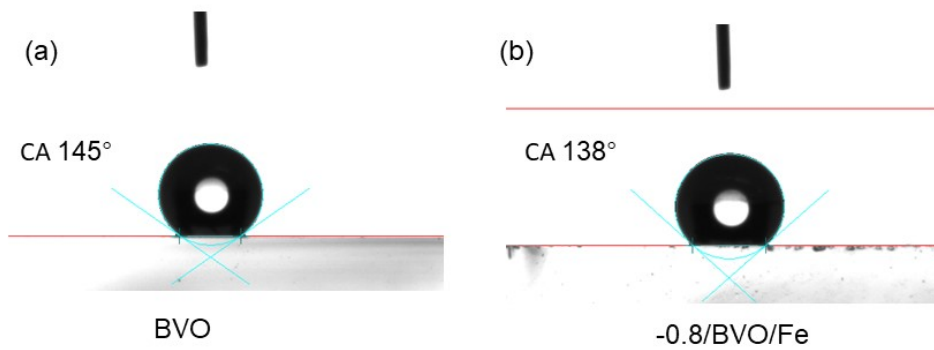


Figure S6. Water contact angle measurement of (a)BVO and (b) -0.8/BVO/Fe.

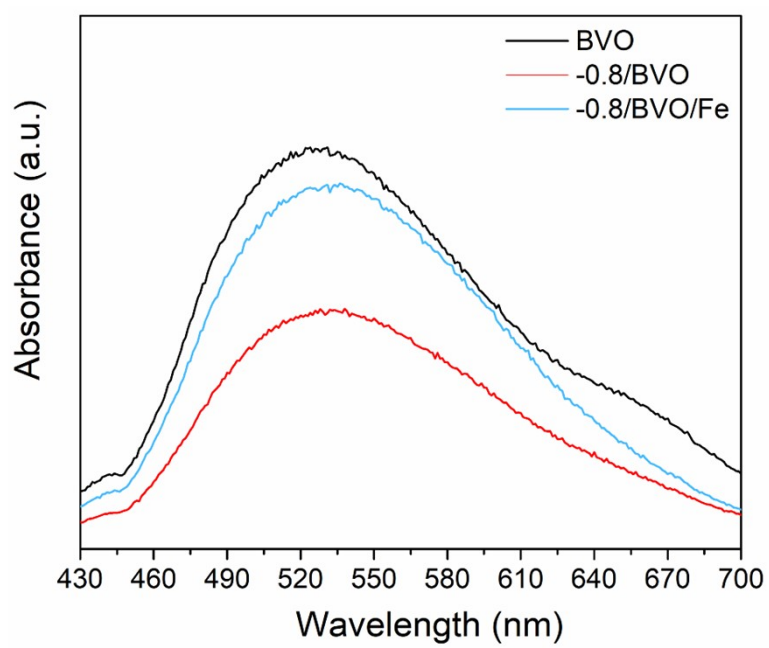


Figure S7. PL emission spectroscopy.

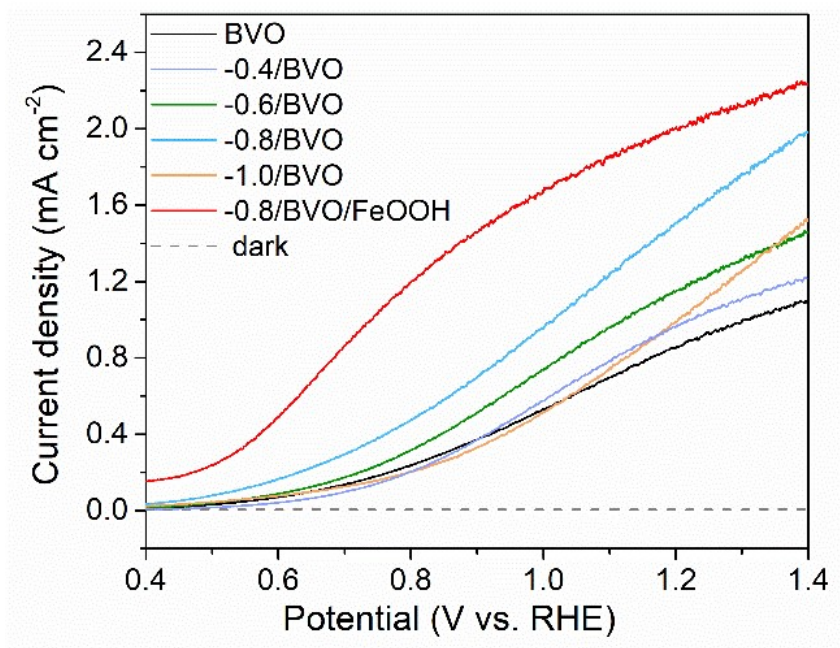


Figure S8. LSV curves of different photoanodes.

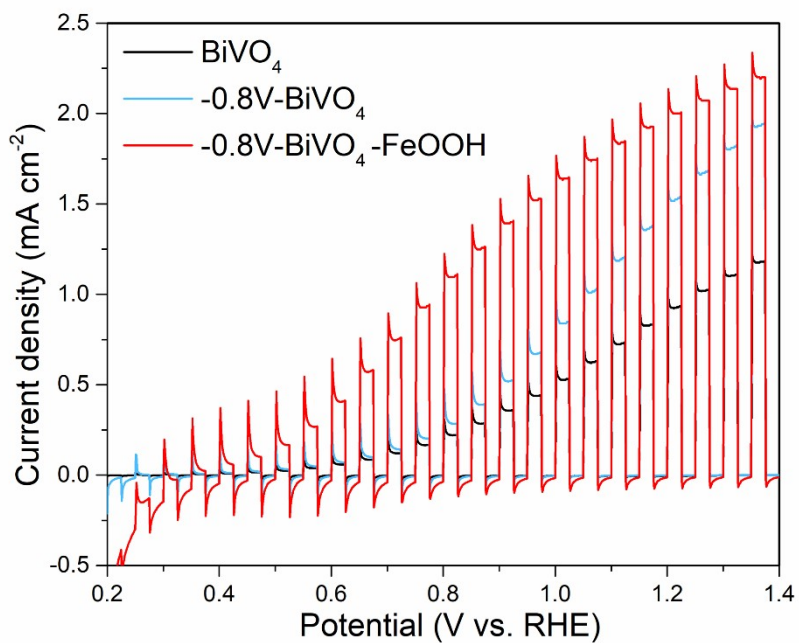


Figure S9. Chopped LSV curves of different photoanodes.

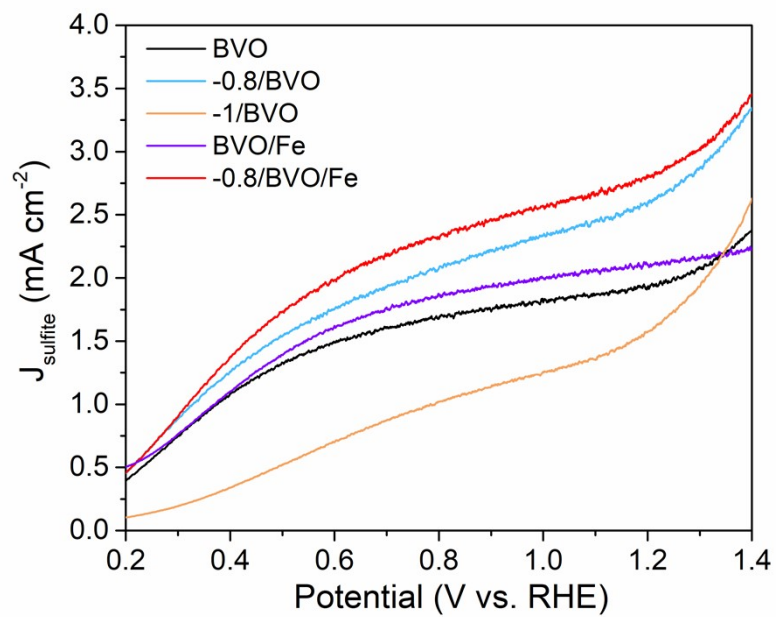


Figure S10. Sulfidation photocurrent with hole scavenger.

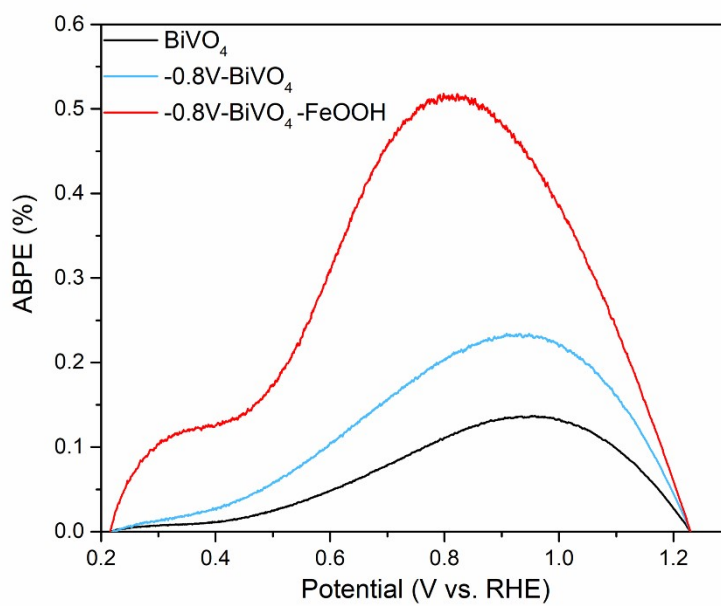


Figure S11. ABPE of the photoanodes.

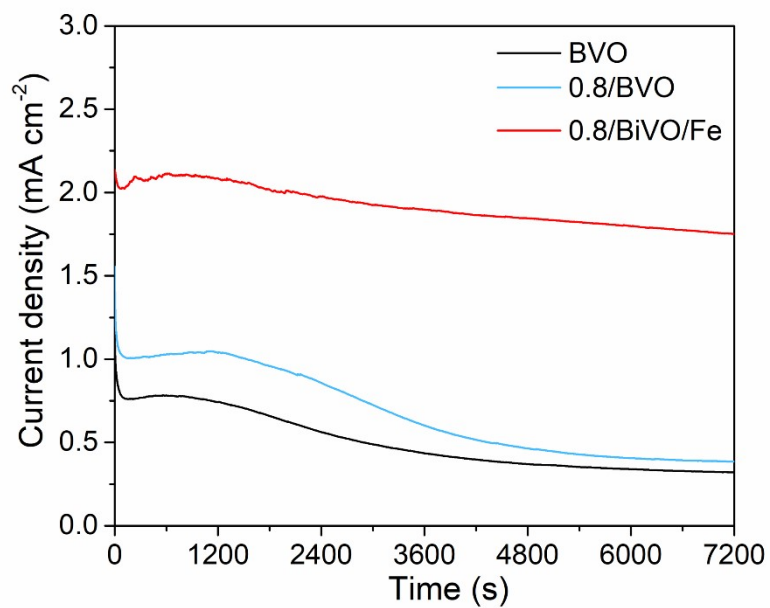


Figure S12. J-t curves the photoanodes measured at 1.23 V_{RHE}

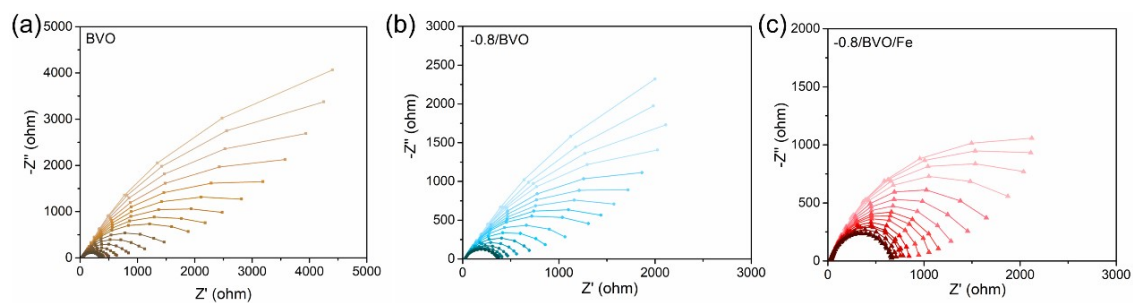


Figure S13. Nyquist plots of photoanodes measured under illumination at 0.4-1.2

V_{RHE} .

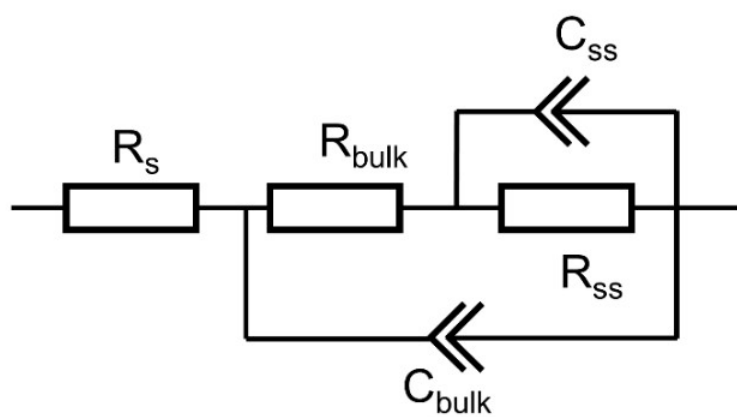


Figure S14. Equivalent circuit used to fit the impedance spectroscopy data for PEIS measurements.

Table S1. Flat band potential and donor density obtained by fitting Mott-Schottky plots.

	flat band potentials	donor density
BVO	0.89 V _{RHE}	7.58×10 ¹⁹
-0.8/BVO	0.81 V _{RHE}	1.03×10 ²⁰
-0.8/BVO/Fe	0.71 V _{RHE}	2.91 ×10 ²⁰

Table S2. Compare the photocurrent density of different BVO based photoanodes at 1.23 V_{RHE}.

Photoanode	J(mA cm ⁻²) at 1.23 V _{RHE}	Electrolyte	pH	Ref.
CoOOH/BiVO ₄	2.4	Na ₂ SO ₄	7	[4]
CoFe-PB/BiVO ₄	0.92	KPi	7	[5]
S-BiVO ₄ /NiO _x	1.7	KPi	7	[6]
Bi _{1-x} VO ₄ /Co-Bi	4.5	KBi	9.5	[7]
TiO ₂ /BiVO ₄	2.1	borate buffer	8	[8]
Mo:BiVO ₄ /CoOOH	1.1	phosphate buffer	7	[9]
-0.8/BiVO ₄ /FeOOH	2.02	Na ₂ SO ₄	6.8	This work

References:

- [1] J. P. Perdew, K. Burke, M. Ernzerhof, *Phys. Rev. Lett.* **1996**, 77, 3865.
- [2] D. Joubert, *Phys. Rev. B: Condens. Matter. Mater. Phys.* **1999**, 59, 1758.
- [3] S. N. Zhevnenko, I. S. Petrov, D. Scheiber, V. I. Razumovskiy, *Acta. Mater.* **2021**,

205, 116565.

- [4] F. S. Hegner, I. Herraiz-Cardona, D. Cardenas-Morcoso, N. López, J. R. Galán-Mascarós, S. Gimenez, *ACS Appl. Mater. Interfaces* **2017**, *9*, 37671.
- [5] B. Zhang, X. Huang, H. Hu, L. Chou, Y. Bi, *J. Mater. Chem. A* **2019**, *7*, 4415.
- [6] S. Gahlawat, P. Schnell, R. Irani, I. Y. Ahmet, L. Choubrac, S. Fiechter, P. P. Ingole, F. F. Abdi, *Sol. RRL* **2022**, *3*.
- [7] Y. Lu, Y. Yang, X. Fan, Y. Li, D. Zhou, B. Cai, L. Wang, K. Fan, K. Zhang, *Adv. Mater.* **2022**, *34*, 1.
- [8] H. Chen, J. Li, W. Yang, S. E. Balaghi, C. A. Triana, C. K. Mavrokefalos, G. R. Patzke, *ACS Catal.* **2021**, *11*, 7637.
- [9] R. Yalavarthi, R. Zbořil, P. Schmuki, A. Naldoni, Š. Kment, *J. Power Sources* **2021**, *483*, 229080.